Research Article

Nan Wang*, Weidong Wen and Haitao Cui

A continuum damage model for fatigue life prediction of 2.5D woven composites

https://doi.org/10.1515/secm-2021-0063
received September 05, 2021; accepted November 11, 2021

Abstract: A new model based on continuum damage mechanics is proposed to predict the fatigue life of 2.5D woven composites. First, a full-cell model reflecting the real microstructure of 2.5D woven composites is established in ANSYS. Subsequently, three independent damage variables are defined in the framework of the composite micromechanics to establish the component constitutive relations associated with damage. The strain energy density release rate and damage evolution equations for the matrix, fiber in yarns, and matrix in yarns are derived. Finally, the proposed model is implemented for fatigue life prediction and damage evolution analysis of 2.5D woven composites at 20 and 180°C. The results show that the numerical results are in good agreement with the relevant experimental results.

Keywords: continuum damage mechanics, 2.5D woven composites, composite micromechanics, fatigue life prediction, damage evolution analysis

Nomenclature

A_{ij}; B_{ij}; C_{ij}	parameters of damage evolution equations
a; b; c	parameters of weft contour curve
A_{w}; A_j	cross-sectional area of weft and warp yarns
k_j; h	parameters of warp contour curve
L_x; L_y; L_z	length, width, and thickness of geometric structure
M_{w}; M_j	arranged density of weft and warp yarns
$D_{0,ij}$	initial damage variables of material components
D_{ij}	damage variables of material components
N_{ij}	fatigue life of material components
N_n; N_{n+1}	fatigue lives in current cycle and next cycle
N_{e}	total number of full-cell model elements
V_{e}	total volume of full-cell model elements
$D_{ij,n}$; $D_{ij,n+1}$	damage variables of last cycle and current cycle
V_{w}; V_j	volume fraction of weft and warp yarns
$s_{ij,fT}$; $s_{ij,mT}$	flexibility coefficients of yarns and matrix
E_{ij}; E_{ij}^{D}	
$\nu_{ij,fT}$; ν_{mT}	Poisson's ratio of yarns and matrix
E_{ffT}; E_{fmT}	elastic modulus of fibers and matrix in yarns
E_{ffT}^{D}; E_{fmT}^{D}	damaged elastic modulus of components in yarns
ρ_j	fiber density
θ	inclination angle of warp yarns
T_{e}	linear density of yarns
$\bar{\varepsilon}$	average strain of unit cell
$\sigma_{ij,fT}$; $\sigma_{ij,mT}$	average stress of yarns and matrix
$\varepsilon_{ij,fT}$; $\varepsilon_{ij,mT}$	average strain of yarns and matrix
N_{w}; N_j	number of weft and warp yarns
T	temperature
V_f	aggregation density of warp yarn
V_{w}	aggregation density (volume fraction) of weft yarn
η_{22}; η_{12}	correction coefficients
ψ	Helmholtz free energy density
W_{D}	average strain energy density
Y	strain energy density release rate
α; β	shear contribution factors
$W_{1\mathrm{w}}$; $W_{2\mathrm{w}}$	width and height of weft yarns
W_{1j}; W_{2j}	width and height of warp yarns
Δx_k^j	distance between opposite planes
$Y_{ij,fT}$	shear strengths of yarns
$X_{ij,fT}$	tension strengths of yarns
X_{ffT}; X_{fmT}	fiber and matrix strengths of yarns

*** Corresponding author: Nan Wang,** Department of Strength and Vibration Engineering, College of Energy and Power Engineering, Nanjing University of Aeronautics and Astronautics, Nanjing 210016, China; State Key Laboratory of Mechanics and Control of Mechanical Structures, Nanjing 210016, China, e-mail: wn0223@nuaa.edu.cn
Weidong Wen, Haitao Cui: Department of Strength and Vibration Engineering, College of Energy and Power Engineering, Nanjing University of Aeronautics and Astronautics, Nanjing 210016, China; State Key Laboratory of Mechanics and Control of Mechanical Structures, Nanjing 210016, China

1 Introduction

In general, 2.5D woven composites represent a special kind of 3D woven composites. Compared with 2D laminated composites, 2.5D woven composites exhibit a more advanced fabric plane and higher delamination resistance; moreover, 2.5D woven composites have a simpler structural configuration than 3D woven composites [1]. Owing to these advantages, 2.5D woven composites are widely used in the domains of aerospace, transportation, sports equipment, civil engineering, among other fields, and present several promising opportunities [2]. Therefore, it is of significance to study the fatigue behavior of angle interlock woven composites for engineering applications.

Many researchers have focused on the mechanical properties and prediction models of angle interlock woven composites [3–9]. Isart et al. [3] adopted three different modeling methods, namely, the idealized method, digital element method, and analytical method, to numerically analyze the global volume fraction and elastic properties of 3D woven composites. The results showed that the first method was faster than the other two methods, although the latter two methods were more accurate in terms of predicting the elastic properties. Based on the Hashin failure criteria and MLT damage model, Warren et al. [4] established a three-dimensional progressive damage model to analyze the damage initiation and propagation of 3D woven composites. Based on the Puck failure criteria, von Mises failure criteria, and quadratic stress criterion for the fiber-matrix interface, Lu et al. [5] established a damage model considering the fiber damage, matrix cracks, and interfacial damage. The model clarified the progressive damage of 2.5D woven composites under quasi-static tension on a mesoscale.

Nevertheless, research on models related to the fatigue life of angle interlock woven composites [10–13] is limited. Stegschuster et al. [10] studied the effect of the z-binder angle of 3D woven composites on the delamination fracture toughness and fatigue strength. The experiments indicated that the fracture toughness and fatigue resistance gradually increased with increasing z-binder volume fraction. Yu et al. [11] used the time-lapse X-ray computed tomography technique to identify the fatigue damage state of 3D woven composites with different fatigue lives. The results showed that the transverse cracks of weft yarns appeared at the initial stage of fatigue life, and the number of transverse cracks steadily increased with increasing fatigue life. Song et al. [12] combined the full-cell model of 2.5D woven composites with the classical progressive damage model which can effectively distinguish the different failure modes of angle interlock woven composites. The fatigue life and damage propagation process of 2.5D woven composites at 20 and 180°C were successfully predicted. Compared with the progressive damage model requiring a mass of experimental data for full material characterization, the continuum damage mechanics model widely used to predict the fatigue life of metallic materials [14–16] needs less experimental data, and it applies phenomenological methods to study the mechanical behavior of fatigue damage. Due to the diversity of components of angle interlock composites, the continuum damage mechanics model has not been effectively applied in the study of fatigue life and damage of 2.5D woven composites.

Therefore, in this study, the microstructure of 2.5D woven composites was examined, and a full-cell model for fatigue damage analysis was established. Based on the full-cell finite element model, the micromechanics of composites and continuum damage mechanics were introduced, and a model to predict the fatigue life of 2.5D woven composite on the microscale was established. Finally, the fatigue damage process and fatigue life of 2.5D woven composites at different temperatures were predicted and analyzed.

2 Geometric structure and finite element model of 2.5D woven composites

2.1 Geometric structure of 2.5D woven composites

Layer-to-layer interlock is one of the most typical structures of 2.5D woven composites. The microstructure of warp yarns, weft yarns, and resin matrix is shown in Figure 1.

According to the early literature, weft cross sections are of racetrack, rectangular, and convex lens types [17–19]. Figure 1(a) shows that under the mutual extrusion of the warp yarn, the cross section of the weft yarn exhibits a bulge in the middle that is sharp at both ends, which conforms to the assumption of a convex lens. A warp yarn can be divided into an enveloping weft section and a linear connection section. Figure 1(b) shows that the weft yarn is basically distributed in a straight orientation, and the cross section of the warp yarn is rectangular.

In addition, the micrograph shows that the outer structure of 2.5D woven composites is considerably different from the inner structure due to the influence of the resin transfer molding (RTM) technology. Therefore, this article adopts the same geometric cross-sectional configuration as in Guo and Song's study [9,12], and the specific dimensions are shown in Figure 2.

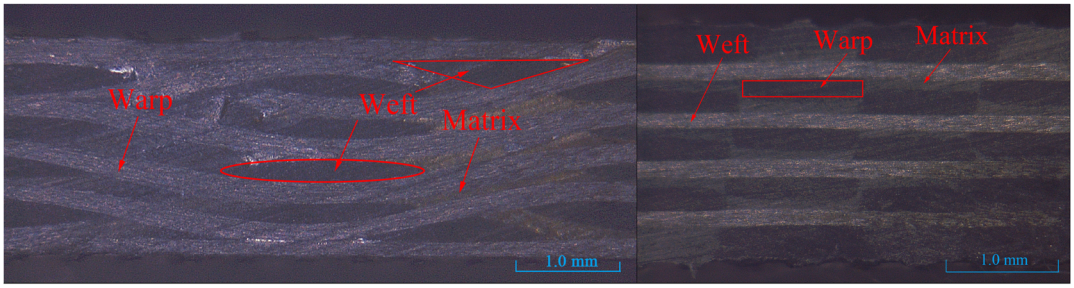

Figure 1: Sectional view of 2.5D woven composites: orientation of (a) warp yarns and (b) weft yarns.

The x-, y-, and z-axes of the rectangular coordinate system in Figure 2 represent the warp, thickness, and weft directions of the geometric structure, respectively. The red curve is the contour curve of the weft yarn, which is described by a quadratic function:

$$f(x) = ax^2 + bx + c, \tag{1}$$

where a, b, and c are unknown parameters. The blue curve is the contour curve of the warp yarn, which is described by a piecewise function:

$$\begin{cases} g(x) = f(x), & 0 \le x < W_{1w}/2, \\ g(x) = k_j x + h, & W_{1w}/2 \le x < L_x/2 - W_{1w}, \end{cases} \tag{2}$$

where k_j and h are unknown parameters. Owing to the influence of the molding technology, the outer warp yarn is flattened, and it is extruded to the inside due to the warp restriction. Therefore, the length of the outer warp yarn should be equal to that of the inner warp yarn.

The overall size of the geometric structure in Figure 2 is obtained as follows:

$$\begin{cases} L_x = 10(N_w - 1)/M_w \\ L_y = 20N_j/M_j, \end{cases} \tag{3}$$

where L_x and L_y are the length and width of the geometric structure (mm), respectively. M_w and M_j represent the weft and warp arranged density (tows per cm), respectively. N_w denotes the number of weft yarns at a given height, and N_j denotes the number of warp pairs in a single layer.

The geometric dimensions of the rectangular cross section of the warp can be calculated, using the following equation:

$$\begin{cases} A_j = \dfrac{T_e}{1{,}000\rho_j V_j} \\ W_{1j} = \dfrac{10}{M_j} \\ W_{2j} = \dfrac{A_j}{W_{1j}}, \end{cases} \tag{4}$$

where A_j is the cross-sectional area of the warp yarn (mm^2), and T_e is the linear density of the yarn (g/km). ρ_j is the fiber density (g/cm^3), and V_j is the aggregation density (volume fraction) of the warp yarn. W_{1j} and W_{2j} represent the width and height of the cross section of the warp yarn, respectively.

The cross-sectional geometric dimensions of the weft and unknown parameters of $f(x)$ and $g(x)$ can be calculated, using the following method:

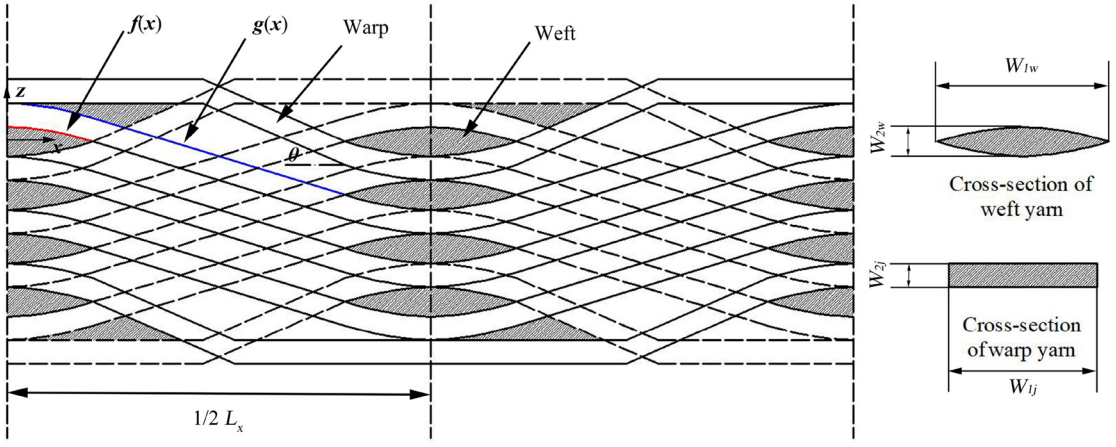

Figure 2: Geometric structure of 2.5D woven composites.

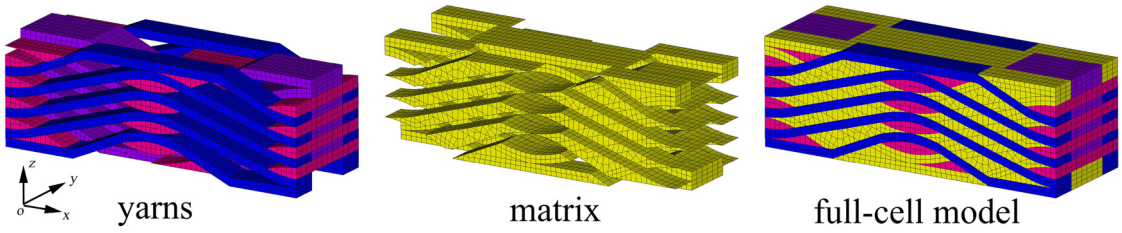

Figure 3: Finite element model of 2.5D woven composites.

$$W_{2w} = \frac{L_z - (N_h + 1)W_{2j}}{N_h - 2}, \tag{5}$$

where L_z is the thickness of the geometric structure (mm), N_h is the number of weft yarns in the thickness direction, and $N_h - 2$ reflects the extrusion effect of the RTM technology in the composites. To obtain the cross-sectional width (W_{1w}) of the weft yarn, the slope k_j of the linear connection section of the warp yarn, and the unknown parameters (a, b, and c) of $f(x)$, five equations must be simultaneously solved. The simultaneous equations are as follows:

$$\begin{cases} c = \dfrac{W_{2w}}{2}, \\ 0 = a\left(\dfrac{W_{1w}}{2}\right)^2 + b\left(\dfrac{W_{1w}}{2}\right) + c, \\ f(x)'|_{x=W_{1w}/2} = k = \tan(\pi - \theta) = 2a\dfrac{W_{1w}}{2} + b, \\ \tan\theta = \dfrac{W_{2j} + W_{2w} + W_{2j}\cos\theta}{L_x/2 - W_{1w} - W_{2j}\sin\theta}, \\ A_w = \dfrac{T_e}{1{,}000\rho V_w} = 4\displaystyle\int_0^{W_{1w}/2} (ax^2 + bx + c)dx \\ \quad = \dfrac{a}{6}{W_{1w}}^3 + \dfrac{b}{2}{W_{1w}}^2 + 2cW_{1w}, \end{cases} \tag{6}$$

where θ is the inclination angle of the warp yarn, A_w is the cross-sectional area of the weft yarn (mm^2), and V_w is the aggregation density (volume fraction) of the weft yarn.

2.2 Full-cell finite element model of 2.5D woven composites

The full-cell finite element model is the basis of fatigue damage analysis of 2.5D woven composites, and its rationality directly affects the accuracy of prediction. In this study, the UG software is used to establish the geometric model of 2.5D woven composites, and HyperMesh software is used for meshing. The periodic boundary conditions of the full-cell model are accomplished through the nodal displacement constraint equations in ANSYS software. The positions of nodes on the parallel planes of the full-cell model have a one-to-one correspondence. To ensure the continuity of the stress and displacement in the structure, the contact areas of the resin matrix, warp yarns, and weft yarns have the same nodes. The finite element full-cell model of the 2.5D woven composites is shown in Figure 3.

Xia et al. [20] proposed an explicit unified form for periodic boundary conditions and proved that the continuity of deformation and stress can be simultaneously satisfied in the unit cell model. The periodic boundary condition can be expressed as:

$$u_i^{j+} - u_i^{j-} = \bar{\varepsilon}\Delta x_k^j \ (i, k = x, y, z), \tag{7}$$

where the superscripts $j+$ and $j-$ represent the positive and negative areas of the jth opposite units, respectively. $\bar{\varepsilon}$ is the average strain of the unit cell, and Δx_k^j is the distance between opposite planes.

For the full-cell model used in this article, it is necessary to ensure that the macroscopic stress in each principal direction is the same as the external load in the fatigue life prediction. The macroscopic stress in each principal direction is obtained, using the volume average method:

$$\sigma_{ij} = \frac{1}{V_e}\sum_{k=1}^{N_e}\sigma_{ijk}V_k, \tag{8}$$

where N_e is the total number of full-cell model elements, σ_{ijk} is the stress of the kth element in the ij direction, V_k is the volume of the kth element, and V_e is the total volume of the full-cell model.

3 Life prediction model of 2.5D woven composites

3.1 Component constitutive relations associated with damage

Based on the full-cell model in this article, 2.5D woven composites can be considered to be composed of the resin matrix and yarns with a relatively complex orientation.

Fiber yarns are generally considered transversely isotropic materials, which are composed of matrix and fibers. The constitutive relation of the yarns at T°C can be expressed as follows:

$$\varepsilon_{ij,fT} = \begin{bmatrix} s_{11,fT} & s_{12,fT} & s_{12,fT} & 0 & 0 & 0 \\ s_{12,fT} & s_{22,fT} & s_{23,fT} & 0 & 0 & 0 \\ s_{12,fT} & s_{23,fT} & s_{22,fT} & 0 & 0 & 0 \\ 0 & 0 & 0 & 2(s_{22,fT} - s_{23,fT}) & 0 & 0 \\ 0 & 0 & 0 & 0 & s_{66,fT} & 0 \\ 0 & 0 & 0 & 0 & 0 & s_{66,fT} \end{bmatrix} \times \sigma_{ij,fT}, \tag{9}$$

$$\begin{cases} s_{11,fT} = \dfrac{1}{E_{11,fT}}, \\ s_{22,fT} = \dfrac{1}{E_{22,fT}}, \\ s_{12.fT} = -\dfrac{\nu_{12,fT}}{E_{11,fT}}, \\ s_{23,fT} = -\dfrac{\nu_{23,fT}}{E_{22,fT}}, \\ s_{66,fT} = \dfrac{1}{G_{12,fT}}, \end{cases} \tag{10}$$

where subscripts $i, j = 1, 2, 3$, and the 1-axis is parallel to the fiber. The 2- and 3-axes are perpendicular to the fiber. $s_{ij,fT}$ is the flexibility coefficient of fiber yarns at T°C. $E_{ij,fT}$, $G_{ij,fT}$, and $\nu_{ij,fT}$ are the elastic moduli, shear moduli, and Poisson's ratio of the yarns at T°C, respectively. The resin matrix is an isotropic material, and its constitutive relation at T°C can be expressed as follows:

$$\varepsilon_{ij,mT} = \begin{bmatrix} s_{11,mT} & s_{12,mT} & s_{12,mT} & 0 & 0 & 0 \\ s_{12,mT} & s_{11,mT} & s_{12,mT} & 0 & 0 & 0 \\ s_{12,mT} & s_{12,mT} & s_{11,mT} & 0 & 0 & 0 \\ 0 & 0 & 0 & 2(s_{11,mT} - s_{12,mT}) & 0 & 0 \\ 0 & 0 & 0 & 0 & 2(s_{11,mT} - s_{12,mT}) & 0 \\ 0 & 0 & 0 & 0 & 0 & 2(s_{11,mT} - s_{12,mT}) \end{bmatrix} \times \sigma_{ij,mT}, \tag{11}$$

$$\begin{cases} s_{11,mT} = \dfrac{1}{E_{mT}}, \\ s_{12,mT} = -\dfrac{\nu_{mT}}{E_{mT}}, \end{cases} \tag{12}$$

where $s_{ij,fT}$, E_{mT}, and ν_{mT} denote the flexibility coefficient, elastic modulus, and Poisson's ratio of the resin matrix at T°C, respectively.

The mechanical properties, failure mechanism, and fatigue damage evolution process of the fibers and matrix in yarns, and resin matrix of 2.5D woven composites are different. Therefore, the damage vector is introduced to characterize the damage degree of 2.5D woven composites with cyclic loading:

$$D_{ij} = \frac{E_{ij} - E_{ij}^{\mathrm{D}}}{E_{ij}}, \tag{13}$$

where E_{ij} and E_{ij}^{D} denote the elastic moduli of undamaged and damaged materials, respectively. The subscripts $ij = ffT, fmT, mT$ represent the fibers in yarns, matrix in yarns, and resin matrix of 2.5D woven composites at T°C, respectively.

According to the theory of damage mechanics and micromechanics of composite materials, the elastic moduli of the yarns with damage in 2.5D woven composites is characterized by the fiber and matrix elastic modulus [21]:

$$E_{11,fT}^{D} = (1 - D_{ffT})E_{ffT}V_f + (1 - D_{fmT})E_{fmT}(1 - V_f), \tag{14}$$

$$E_{22,fT}^{D} = (1 - D_{fmT})E_{fmT}\frac{(1 - D_{ffT})E_{22,ffT} + \eta_{22}[V_f(1 - D_{ffT})E_{22,ffT} + (1 - V_f)(1 - D_{fmT})E_{fmT}]}{(1 - D_{ffT})E_{22,ffT}(1 - V_f) + (1 - D_{fmT})E_{fmT}V_f + \eta_{22}(1 - D_{fmT})E_{fmT}}, \tag{15}$$

$$G_{12,fT}^{D} = (1 - D_{fmT})G_{fmT}\frac{(1 - D_{ffT})G_{12,ffT} + \eta_{12}[V_f(1 - D_{ffT})G_{12,ffT} + (1 - V_f)(1 - D_{fmT})G_{mT}]}{(1 - D_{ffT})G_{12,ffT}(1 - V_f) + (1 - D_{fmT})G_{mT}V_f + \eta_{12}(1 - D_{fmT})G_{mT}}, \tag{16}$$

where V_f is the aggregation density in yarns, and η_{22} and η_{12} are correction coefficients. The elastic modulus of the resin matrix with damage in 2.5D woven composites is

$$E_{mT}^{D} = (1 - D_{mT})E_{mT}, \tag{17}$$

3.2 Damage evolution equation

Continuum damage mechanics is used to derive the damage evolution equation of component damage variables. The Helmholtz free energy density (ψ) of

anisotropic damage materials is a convex function of its observable and internal variables [22], which can be expressed as

$$\psi = \psi(\varepsilon_{ij,ffT}, \varepsilon^{p}_{ij,ffT}, \varepsilon_{ij,fmT}, \varepsilon^{p}_{ij,fmT}, \varepsilon_{ij,mT}, \varepsilon^{p}_{ij,mT}, T, \boldsymbol{\alpha}, \gamma, \boldsymbol{D}), \tag{18}$$

where ε, ε^{p}, $\boldsymbol{\alpha}$, and γ denote the total strain tensor, plastic strain tensor, back strain tensor, and damage cumulative plastic strain of the material components, respectively. In this study, the yarns and resin matrix of 2.5D woven composites (T300/QY8911-IV) are brittle materials, and the experimental temperature is maintained at a constant value. Therefore, the Helmholtz free energy density is equal to the average strain energy density (W_D) of damaged materials, which can be expressed as

$$W_D = \frac{1}{2\rho}[\sigma_{ij,ffT}\varepsilon_{ij,ffT} + \sigma_{ij,fmT}\varepsilon_{ij,fmT} + \sigma_{ij,mT}\varepsilon_{ij,mT}], \tag{19}$$

where ρ is the material density. The strain energy density release rate (Y) defined by the thermodynamic associated variable is derived from the Helmholtz free energy density:

$$\begin{cases} Y_{ffT} = \rho\dfrac{\partial W_D}{\partial D_{ffT}} = \dfrac{\sigma_{ij,ffT}\varepsilon_{ij,ffT}}{2(1 - D_{ffT})}, \\ Y_{fmT} = \rho\dfrac{\partial W_D}{\partial D_{fmT}} = \dfrac{\sigma_{ij,fmT}\varepsilon_{ij,fmT}}{2(1 - D_{fmT})}, \\ Y_{mT} = \rho\dfrac{\partial W_D}{\partial D_{mT}} = \dfrac{\sigma_{ij,mT}\varepsilon_{ij,mT}}{2(1 - D_{mT})}, \end{cases} \tag{20}$$

where the subscripts $ij = ffT, fmT, mT$, and A_{ij}, B_{ij}, and C_{ij} are the unknown parameters of the damage evolution equation. By substituting equation (20) into equation (21), the damage evolution equation of the yarn fibers, yarn matrix, and resin matrix of 2.5D woven composites can be obtained:

$$\begin{cases} \dfrac{\mathrm{d}D_{ffT}}{\mathrm{d}N} = \dfrac{A_{ffT}}{(2E_{ffT})^{B_{ffT}}} \cdot \dfrac{\sigma_{ij,ffT}^{2B_{ffT}}}{(1 - D_{ffT})^{2B_{ffT}+C_{ffT}}} \\ \dfrac{\mathrm{d}D_{fmT}}{\mathrm{d}N} = \dfrac{A_{fmT}}{(2E_{fmT})^{B_{fmT}}} \cdot \dfrac{\sigma_{ij,fmT}^{2B_{fmT}}}{(1 - D_{fmT})^{2B_{fmT}+C_{fmT}}} \\ \dfrac{\mathrm{d}D_{mT}}{\mathrm{d}N} = \dfrac{A_{mT}}{(2E_{mT})^{B_{mT}}} \cdot \dfrac{\sigma_{ij,mT}^{2B_{mT}}}{(1 - D_{mT})^{2B_{mT}+C_{mT}}}. \end{cases} \tag{22}$$

Due to the randomness of fiber distribution in fiber yarns, the true stress of the fiber and matrix in yarns is difficult to obtain. Therefore, the component equivalent stress of the yarn fibers, yarn matrix, and resin matrix of 2.5D woven composites is defined to replace the true stress. The composite component failure criteria (Hashin failure criteria [25]) can be used to define the component equivalent stress of the fiber and matrix in yarns. Due to the complex stress of the pure resin matrix, the von Mises failure criteria can be used to define the component equivalent stress of the resin matrix. The specific form is as follows:

$$\begin{cases} \sigma_{eqv,ffT} = X_{ffT}\sqrt{\left(\dfrac{\sigma_{11,fT}}{X_{11,fT}}\right)^2 + \alpha\left(\dfrac{\sigma_{12,fT}}{Y_{12,fT}}\right)^2 + \alpha\left(\dfrac{\sigma_{13,fT}}{Y_{13,fT}}\right)^2}, \\ \sigma_{eqv,fmT} = X_{fmT}\sqrt{\left(\dfrac{\sigma_{22,fT} + \sigma_{33,fT}}{X_{22,fT}}\right)^2 + \beta\dfrac{\sigma_{23,fT}{}^2 - \sigma_{22,fT}\sigma_{32,fT}}{Y_{23,fT}{}^2} + \beta\left(\dfrac{\sigma_{12,fT}}{Y_{12,fT}}\right)^2 + \beta\left(\dfrac{\sigma_{13,fT}}{Y_{13,fT}}\right)^2}, \\ \sigma_{eqv,mT} = \sqrt{\dfrac{1}{2}(\sigma_{11,mT} - \sigma_{22,mT})^2 + \dfrac{1}{2}(\sigma_{22,mT} - \sigma_{33,mT})^2 + \dfrac{1}{2}(\sigma_{11,mT} - \sigma_{33,mT})^2 + 3(\tau_{12,mT}^2 + \tau_{13,mT}^2 + \tau_{23,mT}^2)}, \end{cases} \tag{23}$$

The damage evolution equation can be derived from the dissipative potential function, which is a convex function of the strain energy density release rate. The works of literature [23,24] assume that the damage evolution equation of composites is a power exponential form of Y, which is expressed as

$$\frac{\mathrm{d}D_{ij}}{\mathrm{d}N} = \frac{A_{ij}Y_{ij}^{B_{ij}}}{(1 - D_{ij})^{C_{ij}}}, \tag{21}$$

where X_{ffT} and X_{fmT} are the fiber and matrix strengths of the yarns, respectively. $X_{11,fT}$ and $X_{22,fT}$ are the longitudinal and transverse tension strengths of the yarns, respectively. $Y_{12,fT}$, $Y_{13,fT}$, and $Y_{23,fT}$ are the shear strengths of the yarns in the material coordinate system. α and β are the shear contribution factors. By substituting equation (23) into equation (22), the damage evolution equation for the fatigue life prediction of 2.5D woven composites can be obtained.

4 Identification of the parameters of the life prediction model

4.1 Process of parameter identification

Separate variable integration of the damage evolution equation of 2.5D woven composites can be performed as follows:

$$\int_0^{N_{ij}} \mathrm{d}N = \int_{D_{0,ij}}^{1} \frac{(2E_{ij})^{B_{ij}}}{A_{ij}} \cdot \frac{(1 - D_{ij})^{2B_{ij}+C_{ij}}}{\sigma_{\mathrm{eqv},ij}^{2B_{ij}}}, \tag{24}$$

where $D_{0,ij}$ is the initial damage variable of the material component, usually set as 0, and N_{ij} is the fatigue life of the material component. By integration of equation (24) from $D_{0,ij} = 0$ to $D_{ij} = 1$, the fatigue life prediction model of 2.5D woven composites can be obtained:

$$\sigma_{\mathrm{eqv},ij}^{2B_{ij}} N_{ij} = \frac{(2E_{ij})^{B_{ij}}}{A_{ij}(2B_{ij} + C_{ij} + 1)}(1 - D_{0,ij})^{2B_{ij}+C_{ij}+1}, \tag{25}$$

To identify the model parameters, the residual stiffness and fatigue life of the yarn fibers and yarn matrix should be obtained by the mechanical property experiment of the yarns. However, it is difficult to directly research the transverse and shear mechanical properties of the yarns, and the experimental conditions are not fully available. Therefore, the mechanical properties of the yarns are obtained by composite laminates with the same fiber volume fraction.

The equation (26) is a relation between normalized stress and logarithmic fatigue life of composite laminates considering the effect of fiber volume fraction:

$$\frac{\sigma_{\mathrm{eqv},ij}}{X_{ij}} = k_{ij} \log_{10}(N_{ij}) + m_{ij}(1 - V_f)^{n_{ij}}, \tag{26}$$

where the subscripts $ij = ffT, fmT, mT$, and k_{ij}, m_{ij}, and n_{ij} are unknown parameters, which are obtained by fitting the fatigue life experimental data of composite laminates with different fiber volume fractions. When V_f is equal to the fiber volume fraction of the warp yarns, weft yarns, and resin matrix, the fatigue life of the material component can be calculated. Take the logarithm of both sides of equation (25):

$$\log N_{ij} = \log\left[\frac{(2E_{ij})^{B_{ij}}}{A_{ij}(2B_{ij} + C_{ij} + 1)}\right] - 2B_{ij} \log \sigma_{\mathrm{eqv},ij}, \tag{27}$$

The value of the unknown parameter B_{ij} in equation (27) can be determined by the slope of the image curve of the logarithmic fatigue life vs the logarithmic component equivalent stress. Previous studies have shown that the stiffness degradation of composite laminates is related to the normalized fatigue life [26,27]. Therefore, this article uses equation (28) to characterize the normalized residual stiffness of the composite laminates:

$$1 - D_{ij} = \frac{E_{ij}^{\mathrm{D}}}{E_{ij}} = \left(1 - \frac{n_{ij}}{N_{ij}}\right)^{r_{ij}}, \tag{28}$$

where the subscripts $ij = ffT, fmT, mT$. n_{ij}/N_{ij} is normalized component fatigue life and r_{ij} is an unknown parameter, which is obtained by fitting the residual stiffness experimental data of composite laminates with different fiber volume fractions. The derivation of equation (28) can be fitted to obtain the damage evolution rate of the yarn fibers, yarn matrix, and resin matrix. Take the logarithm of both sides of derived equation (25):

$$\log\frac{\mathrm{d}D_{ij}}{\mathrm{d}N_{ij}} = \log\left[\frac{A_{ij}}{(2E_{ij})^{B_{ij}}}(\sigma_{\mathrm{eqv},ij})^{2B_{ij}}\right] + (2B_{ij} + C_{ij}) \log (1 - D_{ij})^{-1}. \tag{29}$$

By calculating the slope and intercept of the image curve of the logarithmic damage evolution rate vs the logarithmic damage variables, the values of the unknown parameters A_{ij} and C_{ij} in equation (29) can be obtained.

4.2 Characterization of material and specimen

The 2.5D woven composites and laminated composites in this study are composed of carbon fiber yarns (T300) including 3 K filaments per bundle and resin matrix (QY8911-IV) with a glass transition temperature of 256°C. At 180°C, the temperature does not significantly affect the mechanical properties of the fiber, although it considerably influences the mechanical properties of the resin matrix. The mechanical properties of the fiber and matrix at 20 and 180°C are shown in Table 1.

According to the standard of ASTM D3479 [29], the nominal dimensions of the 2.5D woven composite specimens are designed as 300 mm × 25 mm × 1.95 mm, and the length of end tabs on both sides is 50 mm, as shown in Figure 4.

All specimens were weaved by the institute of composite materials of TianGong University and molded by RTM technology at the Aerospace Research Institute of Material & Processing Technology in China. The specific molding process can refer to the literature [30]. The woven parameters of 2.5D woven composites are shown in Table 2.

Table 1: Mechanical properties of T300-3K and QY8911-IV at 20°C and 180°C [28]

Material	$E_{11,ff20(180)}$	$E_{22,ff20(180)}$	$G_{12,ff20(180)}$	$v_{12,ff20(180)}$	$X_{ff20(180)}$
T300-3K	230 GPa	40 GPa	17 GPa	0.3	3,360 GPa (3,261 GPa)
	$E_{m20(180)}$	$v_{m20(180)}$	$X_{fm20(180)}$		
QY8911-IV	4.16 GPa (2.5 GPa)	0.358	68.28 GPa (31.87 GPa)		

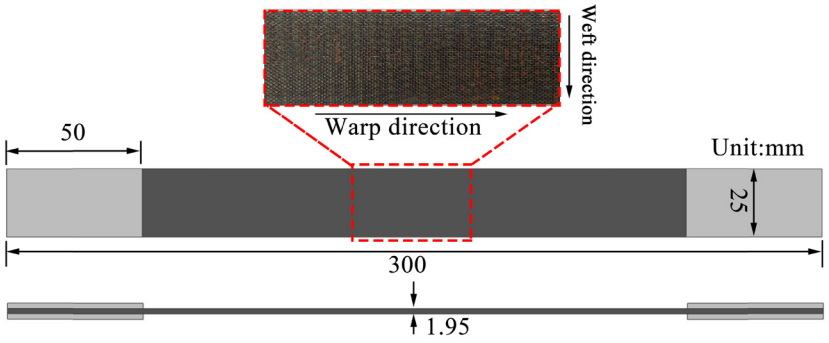

Figure 4: The specific geometric dimensions of the specimen.

Substituting the woven parameters in Table 5 into equations (3)–(5), all unknown parameters in the geometric structure can be obtained, as shown in Table 3.

4.3 Identification of the parameters of the yarn fiber damage evolution equation

Since the ratio of E_{ffT}/E_{fmT} is extremely large, the stiffness degradation of the $[0]_n$ unidirectional ply can be considered as that of the yarn fibers. Therefore, the unknown parameters of the yarn fiber damage evolution equation are fitted, using the tension–tension fatigue experimental results of the $[0]_n$ unidirectional plies with fiber volume fractions of 47.20, 51.89, 62.97, and 64.32%.

The tension–tension fatigue experiment of the $[0]_n$ unidirectional ply is based on the ASTM D3479 standard [29], the loading frequency is 10 Hz, and the stress ratio is 0.1. Figure 5 shows the experimental data and fitting curves of the normalized stress vs the logarithmic fatigue life of $[0]_n$ unidirectional plies with different fiber volume fractions at different temperatures.

The experimental data in Figure 5 are inserted into equation (26) and fitted, using the least square method to obtain the unknown parameters k_{ffT}, m_{ffT}, and n_{ffT}. In the figure, the fitting curves of the warp and weft fibers at 20°C are wine red and purple, and those at 180°C are olive green and cyan blue. The experimental data and fitting curves of the normalized residual stiffness vs the normalized fatigue life of $[0]_n$ unidirectional plies with different fiber volume fractions at different temperatures are shown in Figure 6.

It can be seen from the experimental data in Figure 6 that the residual stiffness of the yarn fiber is mainly affected by temperature, and the least square method is used to fit the unknown parameter r_{ffT} in equation (28) at 20 and 180°C. The corresponding fitting curves at 20 and 180°C are represented by the blue and purple in the figure. Following the method described in Section 4.1, the unknown parameters A_{ffT}, B_{ffT}, and C_{ffT} of the yarn

Table 2: Woven parameters of 2.5D woven composites [30]

Material component	Yarn arranged density (tows/cm)	Number of layers in the weft direction	Yarn sectional area (mm^2)	Fiber aggregation density
Warp yarns	10	5	0.16	0.7
Weft yarns	3.5	6	0.147	0.765

Table 3: Unknown parameters of the geometric structure

Parameter	a	b	c	k_j	h
Value	−0.2383	−0.0342	0.1	−0.3106	0.1801

fiber damage evolution equation can be obtained. The specific values are shown in Table 4.

4.4 Identification of the parameters of the matrix and yarn matrix damage evolution equation

Because the fiber strength of the composites is considerably greater than the strength of the matrix, the matrix of the composites is expected to be damaged first when the matrix direction is loaded. The damage of the fiber at this instant is small and can be ignored. Therefore, the unknown parameters of the matrix and yarn matrix damage evolution equations are fitted by the tension–tension fatigue experimental results of $[\pm45]_n$ cross-ply laminates with fiber volume fractions of 44.4, 52.1, 56.59, and 65%, respectively.

The tension–tension fatigue experiment of $[\pm45]_n$ cross-ply laminates is performed with reference to the ASTM D3479 standard [29]. The loading frequency is 10 Hz. The stress ratio is 0.1. The experimental data and fitting results of $[\pm45]_n$ cross-ply laminates with different fiber volume fractions at different temperatures are shown in Figure 7.

The experimental data in Figure 7 are substituted in equation (26), and the unknown parameters $k_{fmT(mT)}$, $m_{fmT(mT)}$, and $n_{fmT(mT)}$ are obtained, using the least square method. In the figure, the fitting curves of the matrix, warp matrix, and weft matrix at 20°C are purple, wine red, and olive green, and those at 180°C are orange, royal blue, and pink, respectively. The experimental data and fitting curves of the normalized residual stiffness vs the normalized fatigue life of $[\pm45]_n$ cross-ply laminates with different fiber volume fractions at different temperatures are shown in Figure 7.

Considering the experimental data presented in Figure 8, the residual stiffness of the yarn matrix is mainly affected by temperature, and the least square method is used to fit the unknown parameter $r_{fmT(mT)}$ in equation (28) at 20 and 180°C. The fitting curves of the matrix and yarn matrix at 20 and 180°C are the orange and navy blue in the figure. Following the method described in Section 4.1, the unknown

Table 4: Unknown parameters of the yarn fiber damage evolution equation

Temperature (°C)	Material	A_{ffT}	B_{ffT}	C_{ffT}	k_{ffT}	m_{ffT}	n_{ffT}	r_{ffT}
20	Weft fibers	7.33×10^{-21}	10.295	19.42	−0.1005	1.368	−0.02666	0.02438
	Warp fibers	1.26×10^{-20}	10.185	19.64				
180	Weft fibers	8.84×10^{-35}	23.48	−31.56	−0.0411	1.018	−0.00278	0.0610
	Warp fibers	1.04×10^{-34}	23.44	−31.48				

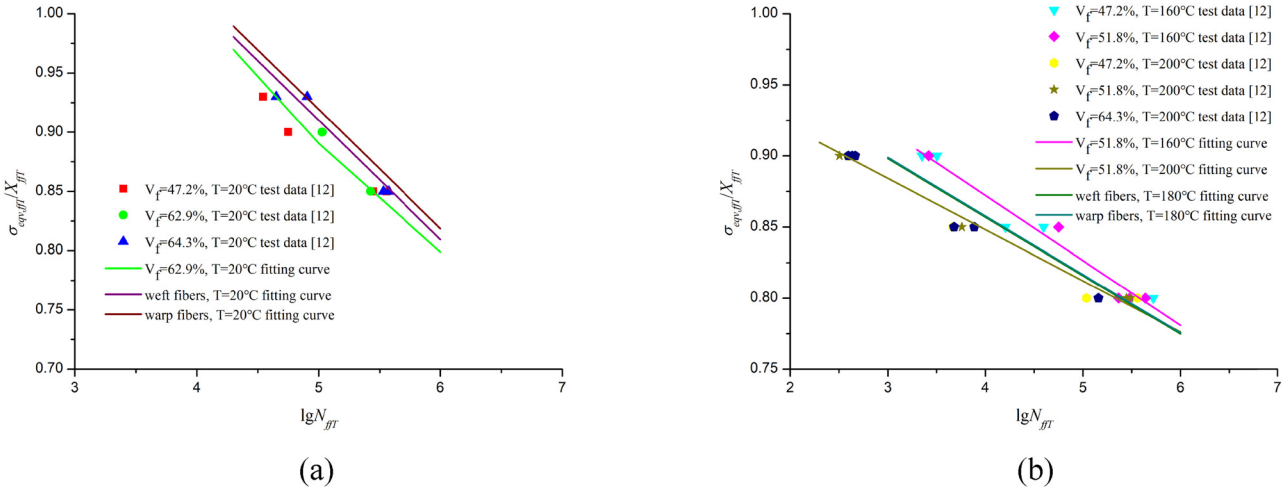

Figure 5: The fitting curve of the normalized stress vs the logarithmic fatigue life of $[0]_n$ unidirectional plies at (a) 20°C and (b) 180°C.

Table 5: Unknown parameters of the yarn matrix damage evolution equation

Temperature (°C)	Material	A_{fmT}	B_{fmT}	C_{fmT}	k_{fmT}	m_{fmT}	n_{fmT}	r_{fmT}
20	Weft matrix	0.1256	11.05	−6.56	−0.0841	0.9776	−0.1356	0.06046
	Warp matrix	0.2093	10.525	−5.51				
180	Weft matrix	0.0867	3.4355	−3.706	−0.2098	0.8518	−0.405	0.2401
	Warp matrix	0.0464	2.6295	−2.094				

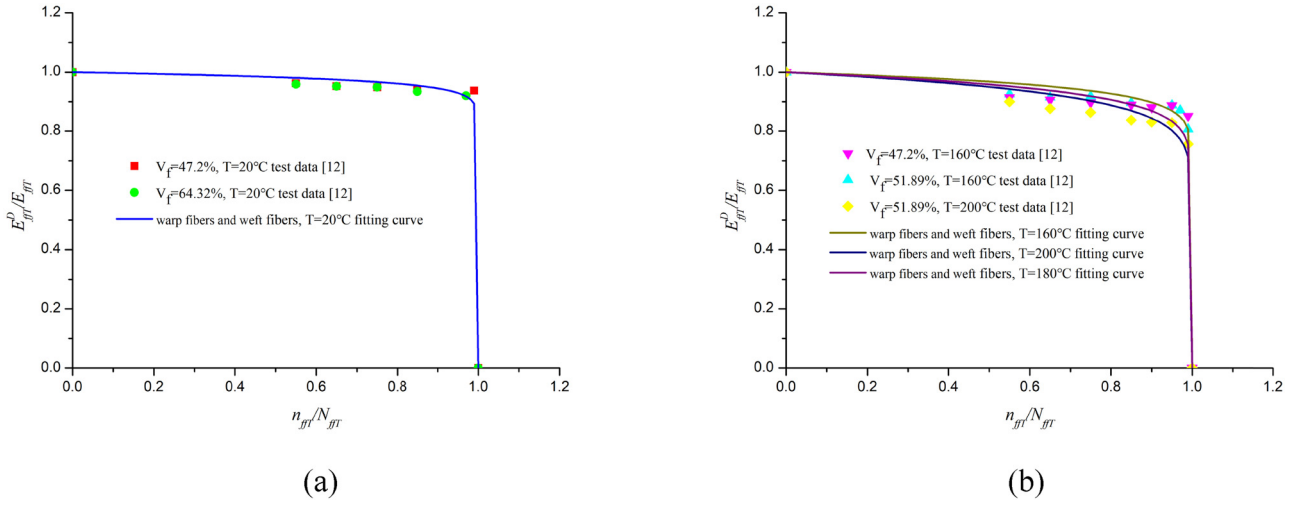

Figure 6: The fitting curve of the normalized residual stiffness vs the normalized fatigue life of $[0]_n$ unidirectional plies at (a) 20°C and (b) 180°C.

parameters $A_{fmT(mT)}$, $B_{fmT(mT)}$, and $C_{fmT(mT)}$ of the yarn matrix and matrix damage evolution equation can be obtained. The specific values are shown in Tables 5 and 6.

5 Results and discussion

5.1 Process of fatigue life prediction

The finite element analysis method is introduced in the fatigue life prediction model of 2.5D woven composites. Based on ANSYS software and APDL language, a program for the fatigue behavior analysis of 2.5D woven composites at different temperatures is developed. The compilation process is shown in Figure 9.

As shown in Figure 9, first the mechanical properties of the warp yarns, weft yarns, and resin matrix are input, and the finite element model of 2.5D woven composites is established with reference to the real geometric structure. After applying periodic boundary conditions, the program enters the life cycle subroutine, in which the cycle increment step is defined as ΔN. To ensure the efficiency and accuracy of the final life prediction, the value of the cycle increment step in this study is $\Delta N = 100$. The fatigue life of the current cycle can be expressed in the following form:

$$N_{n+1} = N_n + \Delta N, \tag{30}$$

where N_n and N_{n+1} represent the fatigue lives in the current cycle and next cycle, respectively. A fatigue load is applied to determine the stress state of each component element in the material coordinate system. In each cycle increment step, the damage variable increment of the yarn fibers, yarn matrix, and resin matrix can be calculated by equation (22), and the damage variable of the current cycle can be expressed in the following form:

$$D_{ij,n} = D_{ij,n-1} + \Delta D_{ij}, \tag{31}$$

where $D_{ij,n}$ and $D_{ij,n+1}$ are the damage variables of the last cycle and current cycle, respectively. Next the stiffness and damage variable values of each component element are updated based on equations (14–16) and (31), and the steps are repeated. When the damage variable of the current cycle of the material component is approximately equal to 1, the material component fails. At this time,

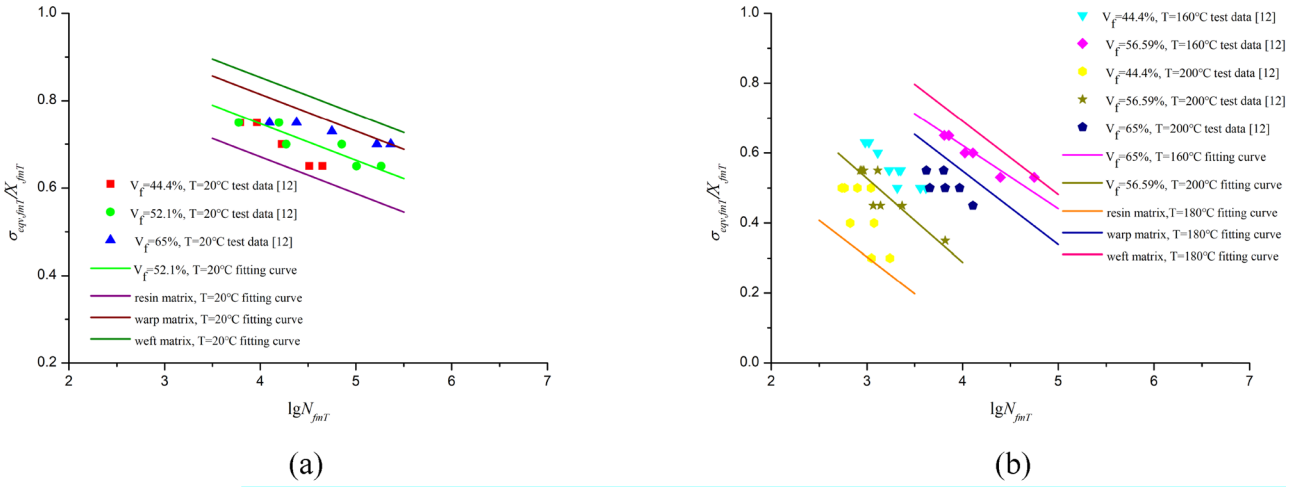

Figure 7: The fitting curve of the normalized stress vs the logarithmic fatigue life of $[\pm 45]_n$ cross-ply laminates at (a) 20°C and (b) 180°C.

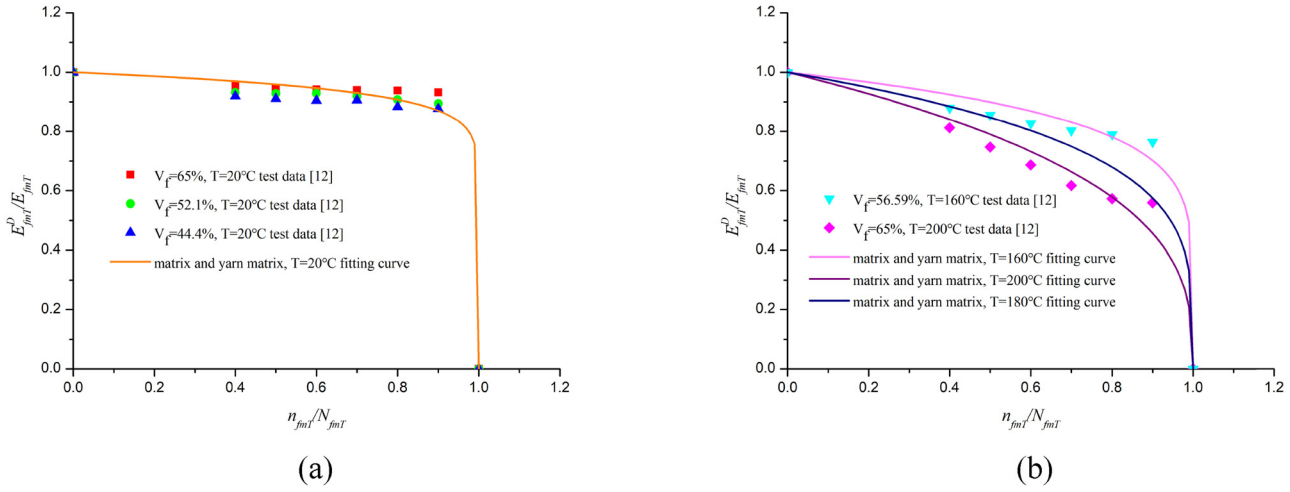

Figure 8: The fitting curve of the normalized residual stiffness vs the normalized fatigue life of $[\pm 45]_n$ cross-ply laminates at (a) 20°C and (b) 180°C.

it is necessary to judge whether the full-cell model is completely damaged. If the percentage of the longitudinal damage elements of the yarns accounts for more than 50% of the total number of warp and weft elements, or the longitudinal damage elements of the yarns extend to the edge of the model, the whole structure is destroyed. The life cycle subroutine is exited, and the current cycle corresponds to the fatigue life of the 2.5D woven composites.

5.2 Predicted fatigue life of 2.5D woven composites

To study the effectiveness of the fatigue life prediction model based on continuum damage mechanics, the longitudinal tension–tension fatigue life of 2.5D (T300/QY8911-IV) woven composites at 20 and 180°C is predicted, and the results are experimentally verified. The loading frequency and stress ratio of 2.5D woven composites in the

Table 6: Unknown parameters of the matrix damage evolution equation

Material	Temperature (°C)	A_{mT}	B_{mT}	C_{mT}	k_{mT}	m_{mT}	n_{mT}	r_{mT}
Matrix	20	0.8240	8.55	−1.56	−0.0841	0.9776	−0.1356	0.06046
	180	0.1470	1.578	0.009	−0.2098	0.8518	−0.405	0.2401

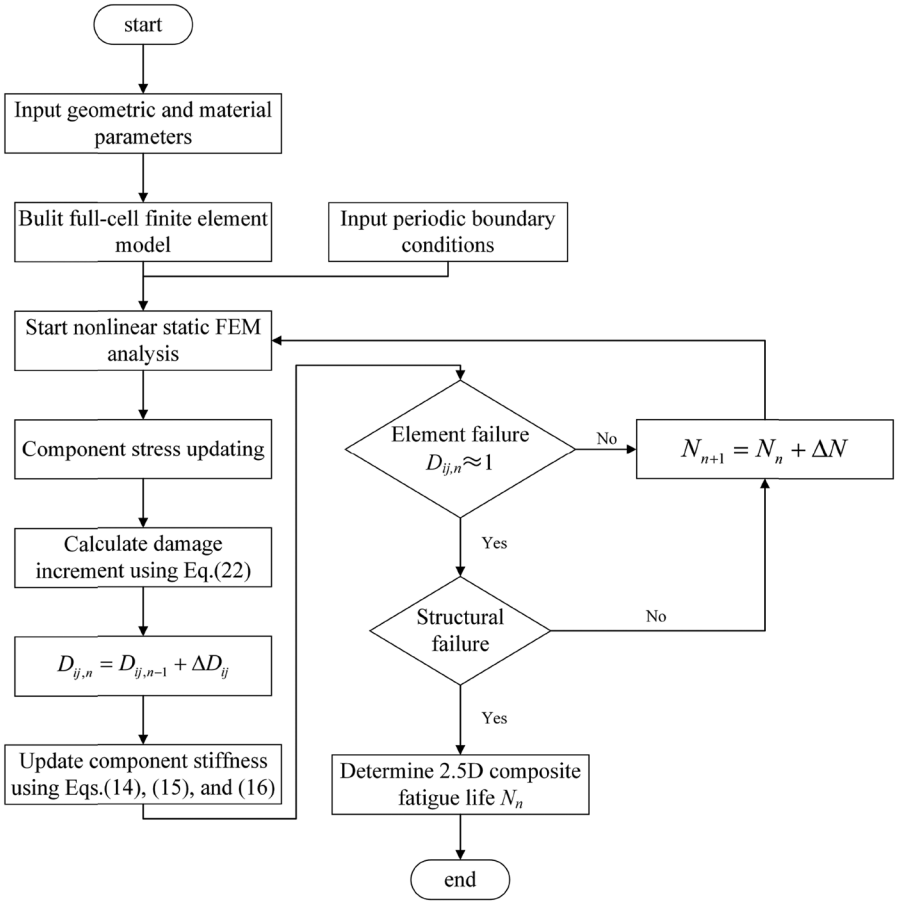

Figure 9: Flowchart for the fatigue life prediction of 2.5D woven composites.

fatigue experiment are 10 Hz and 0.1, respectively. The fatigue life experimental data of 2.5D woven composites is referenced from Song's study [30]. The experimental and predicted values are compared in Table 7.

Table 7 shows that the predicted logarithmic fatigue life at 20 and 180°C is close to the logarithmic experimental life. The maximum ratios of the predicted life to experimentally obtained life with stress levels of 90, 87, and 80% at 20°C are 1.0427, 1.6080, and 1.6482, respectively, which are within the two-error band. The maximum ratios of the predicted life to experimentally obtained life at 180°C with stress levels of 80, 75, and 73% are 1.6789, 1.3488, and 1.1394, respectively, which are within the two-error band.

In addition, Figure 10 shows the predicted fatigue life of 2.5D woven composites obtained through the proposed model and progressive damage model at 20 and 180°C.

The figure shows that the experimental results are in agreement with the fatigue life predicted by the proposed model and progressive damage model. However, compared with the progressive damage model [12,31], the proposed model only needs the stress-fatigue life and residual stiffness experimental data of the material components when predicting the fatigue life of 2.5D woven composites. Notably, the residual strength experimental data of the material components are not required, which

Table 7: Comparison of the predicted and experimental values of the 2.5D woven composites

Temperature (°C)	Stress level (%)	Testing value (lg N)	Prediction value (lg N)
20	90	3.9686	3.9868
	87	4.0069	4.2355
		4.4418	
	80	4.8688	4.9074
		5.1244	
180	80	2.9689	2.9542
		3.1793	
	75	3.3324	3.4624
		3.4268	
	73	3.6154	3.6721
		3.6352	

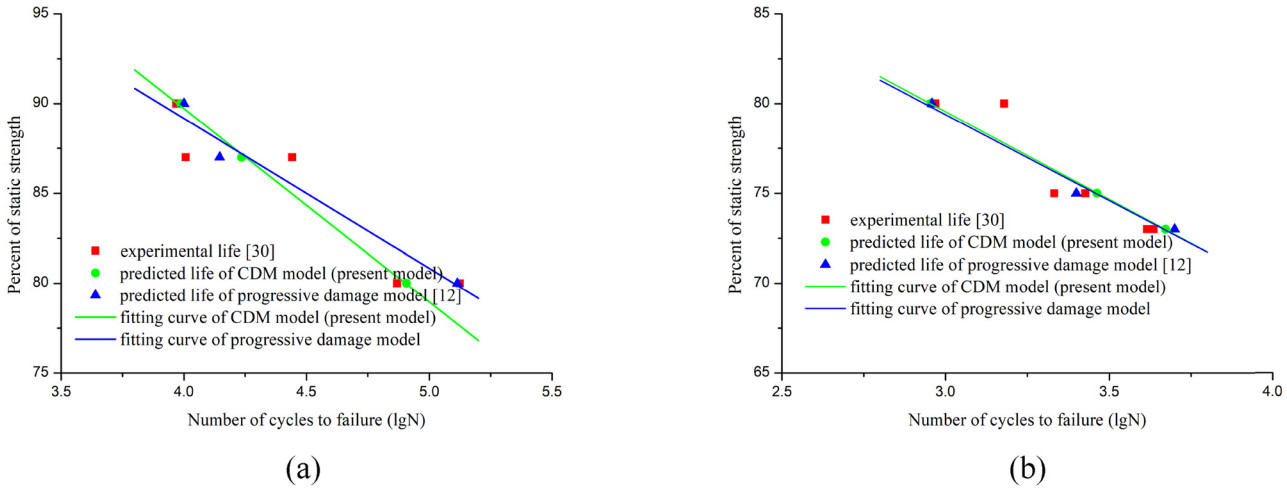

Figure 10: Comparison of fatigue life of 2.5D woven composites predicted using different models and experimental results at (a) 20°C and (b) 180°C.

significantly reduces the testing and time costs. In addition, the progressive damage model assumes that the residual strength is related to the fatigue damage evolution of the material, and the residual stiffness is considered only to update the stiffness matrix of the material. Therefore, the macroscopic stiffness modulus of the material does not correspond to the microscopic damage propagation. The continuum damage mechanics model can solve this problem by constructing the constitutive equation of the material components subjected to damage and establishing the phenomenological damage evolution equation.

5.3 Damage evolution process of 2.5D woven composites

To theoretically study the damage propagation regulation and failure mode in longitudinal tension–tension fatigue loading, the established fatigue life prediction model is used to quantitatively analyze the damage propagation process of 2.5D woven composites with stress levels of 80% at 20 and 180°C. The corresponding results are shown in Figures 11 and 12.

As shown in Figure 11(1)–(3), in the initial stage of fatigue damage propagation at 20°C, the surface and

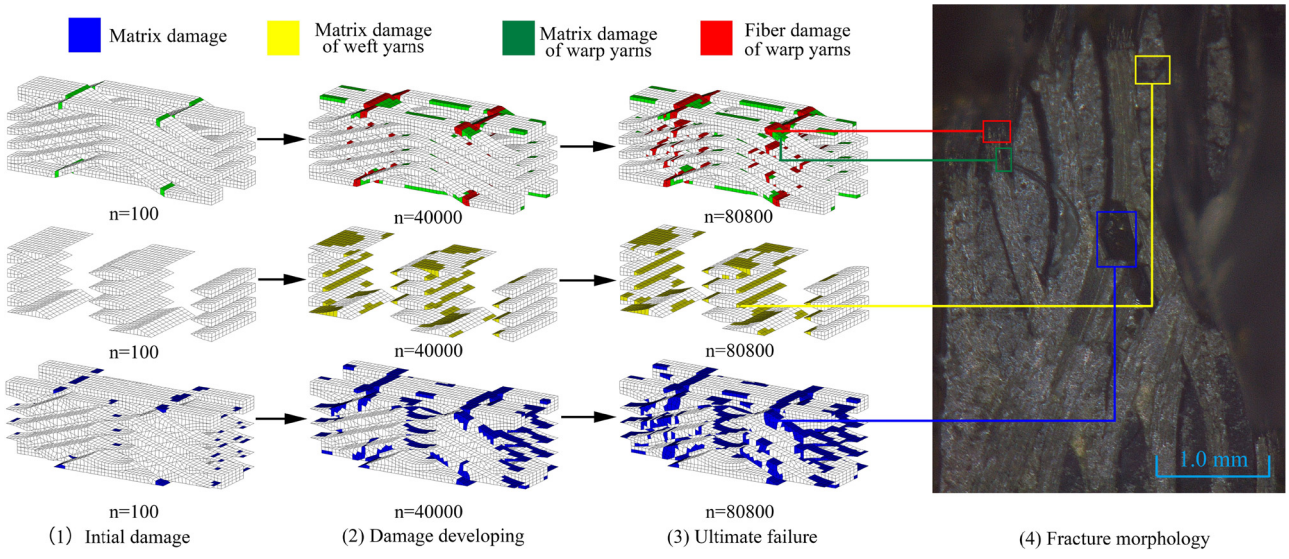

Figure 11: Damage propagation process and experimental fracture morphology of 2.5D woven composites at 20°C.

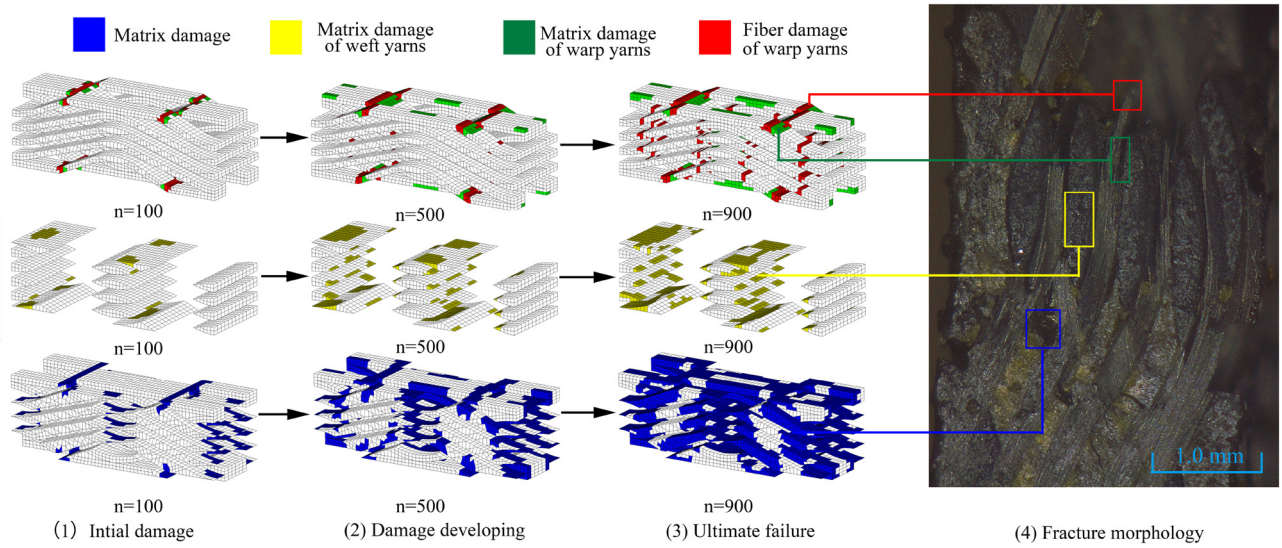

Figure 12: Damage propagation process and experimental fracture morphology of 2.5D woven composites at 180°C.

interior of the 2.5D woven composites are subjected to cracking of the warp matrix and failure damage of the resin matrix. As the number of cycles increases to 40,000, a small amount of weft matrix cracking occurs inside the structure, and a large number of fibers break in the surface warp yarns and expand along the interior of the 2.5D woven composite structure. As the number of cycles increases to 80,800, the fiber fracture at the intersection of the straight and inclined sections of the warp runs through the entire structure. At this time, many resin matrix failures occur, and part of the yarn matrix exhibits cracking damage around the broken warp. According to Figure 12(1)–(3), due to the influence of temperature, fiber breakage occurs on the surface of the warp yarn after 100 cycles, and the other types of damage are intensified as the number of cycles increases. When the number of cycles increases to 900, the fiber fracture in the warp yarn expands to the edge of the structure along the direction perpendicular to the load, and the 2.5D woven composites fail. In addition, Figures 11(4) and 12(4) show photographs of the tension–tension fatigue experimental fractures at 20 and 180°C. The failure mode of the fracture indicates that the final fatigue fracture obtained by the simulation in this study is in agreement with the experimental fracture.

6 Conclusion

A new model to analyze the fatigue damage of 2.5D woven composites is proposed by coupling continuum damage mechanics with composite micromechanics. By defining three independent damage variables, different failure modes (yarn fiber failure, yarn matrix failure, and matrix failure) of 2.5D woven composites are distinguished. According to the fatigue experimental data of $[0]_n$ unidirectional plies and $[\pm 45]_n$ cross-ply laminates with different fiber volume fractions, the unknown parameters associated with the corresponding damage evolution equation are obtained by fitting. Compared with the progressive damage model, the proposed model can predict the fatigue life of 2.5D woven composites using only the stress-fatigue life and residual stiffness experimental data of the material components, thereby reducing the testing and time costs. The fatigue behavior of 2.5D woven composites at 20 and 180°C is studied by performing a numerical simulation and comparing the results with experimental data. The consistency between the simulation and test results demonstrates that the proposed model can effectively predict the fatigue life, damage evolution regulation, and fatigue fracture morphology of 2.5D woven composites.

Funding information: This work was supported by National Science and Technology Major Project (2017-IV-0007-0044) and National Natural Science Foundation of China (52175142).

Conflict of interest: The authors declare no conflict of interest.

References

[1] Mouritz AP, Bannister MK, Falzon PJ, Leong KH. Review of applications for advanced three-dimensional fibre textile composites. Compos A Appl S. 1999;30(12):1445–61.

[2] Mahmood A, Wang X, Zhou C. Modeling strategies of 3D woven composites: a review. Compos Struct. 2011;93(8):1947–63.
[3] Isart N, Said BE, Ivanov DS, Hallett SR, Mayugo JA, Blanco N. Internal geometric modelling of 3D woven composites: a comparison between different approaches. Compos Struct. 2015;132:1219–30.
[4] Warren KC, Roberto AL, Senthil SV, Harun HB, Bayraktar HH. Progressive failure analysis of three-dimensional woven carbon composites in single-bolt, double-shear bearing. Compos B Eng. 2016;84:266–76.
[5] Lu H, Guo L, Liu G, Zhong S, Zhang L, Pan S. Progressive damage investigation of 2.5D woven composites under quasi-static tension. Acta Mech. 2019;230(4):1323–36.
[6] Green SD, Matveev MY, Long AC, Ivanov D, Hallett SR. Mechanical modelling of 3D woven composites considering realistic unit cell geometry. Compos Struct. 2014;118(1):284–93.
[7] Zhang D, Chen L, Wang Y, Sun Y, Jia N, Qian K. Finite element analysis of warp-reinforced 2.5D woven composites based on a meso-scale voxel model under compression loading. Appl Compos Mater. 2017;24(4):911–29.
[8] Tao W, Zhu P, Wang D, Zhao C, Liu Z. Progressive damage modelling and experimental investigation of three-dimensional orthogonal woven composites with tilted binder. J Ind Text. 2020;50(1):70–97.
[9] Guo J, Wen W, Zhang H, Cui H, Song J. Mechanical properties prediction of 2.5D woven composites via voxel-mesh full-cell model. Fiber Polym. 2021;22(7):1899–914.
[10] Stegschuster G, Pingkarawat K, Wendland B, Mouritz AP. Experimental determination of the mode I delamination fracture and fatigue properties of thin 3D woven composites. Compos A Appl S. 2016;84:308–15.
[11] Yu B, Blanc R, Soutis C, Withers PJ. Evolution of damage during the fatigue of 3D woven glass-fibre reinforced composites subjected to tension–tension loading observed by time-lapse X-ray tomography. Compos A Appl S. 2016;82:279–90.
[12] Song J, Wen W, Cui H. Fatigue life prediction model of 2.5D woven composites at various temperatures. Chinese J Aeronaut. 2018;31(2):310–29.
[13] Sun B, Wang J, Wu L, Fang F, Gu B. Computational schemes on the bending fatigue deformation and damage of three-dimensional orthogonal woven composite materials. Com Mater Sci. 2014;91:91–101.
[14] Bhattacharya B, Bruce E. Continuum damage mechanics analysis of fatigue crack initiation. Int J Fatig. 1998;20(9):631–9.
[15] Zhang T, McHugh PE, Leen SB. Finite element implementation of multiaxial continuum damage mechanics for plain and fretting fatigue. Int J Fatig. 2012;44:260–72.
[16] Nadeem AB, Wahab MA. Fretting fatigue damage nucleation under out of phase loading using a continuum damage model for non-proportional loading. Tribol Int. 2018;121:204–13.
[17] Nehme S, Hallal A, Fardoun F, Younes R, Hagege B, Aboura Z, et al. Numerical/analytical methods to evaluate the mechanical behavior of interlock composites. J Compos Mater. 2011;45(16):1699–716.
[18] Rao PM, Walter TR, Sankar B, Subhash G, Yen CF. Analysis of failure modes in three-dimensional woven composites subjected to quasi-static indentation. J Compos Mater. 2014;48(20):2473–91.
[19] Dai S, Cunningham PR. Multi-scale damage modelling of 3D woven composites under uni-axial tension. Compos Struct. 2016;142:298–312.
[20] Xia Z, Zhang Y, Ellyin F. A unified periodical boundary conditions for representative volume elements of composites and applications. Int J Solids Struct. 2003;40(8):1907–21.
[21] Affdl J, Halpin C, Kardos JL. The Halpin–Tsai equations: a review. Polym Eng Sci. 1976;16(5):344–52.
[22] Chaboche JL, Lesne PM. A non-linear continuous fatigue damage model. Fatigue Fract Eng Mater Struct. 1988;11(1):1–17.
[23] Shi W, Hu W, Zhang M. A damage mechanics model for fatigue life prediction of fiber reinforced polymer composite lamina. Acta Mech Solida Sin. 2011;24(5):399–410.
[24] Mohammadi B, Fazlali B, Majd DS. Development of a continuum damage model for fatigue life prediction of laminated composites. Compos A Appl S. 2017;93:163–76.
[25] Hashin Z. Failure criteria for unidirectional fiber composites. J Appl Mech. 1980;47(2):329–34.
[26] Philippidis TP, Vassilopoulos AP. Fatigue of composite laminates under off-axis loading. Int J Fatig. 1999;21(3):253–62.
[27] Mao H, Mahadevan S. Fatigue damage modelling of composite materials. Compos Struct. 2002;58(4):405–10.
[28] Song J, Wen W, Cui H, Liu H, Xu Y. Effects of temperature and fiber volume fraction on mechanical properties of T300/QY8911-IV composites. J Reinf Plast Comp. 2015;34(2):157–72.
[29] Baere ID, Paepegem WV, Quaresimin M, Degrieck J. On the tension–tension fatigue behaviour of a carbon reinforced thermoplastic part I: limitations of the ASTM D3039/D3479 standard. Polym Test. 2011;30(6):625–32.
[30] Song J, Wen W, Cui H. Fatigue behaviors of 2.5D woven composites at ambient and un-ambient temperatures. Compos Struct. 2017;166:77–86.
[31] Shokrieh MM, Lessard LB. Progressive fatigue damage modeling of composite materials, part II: material characterization and model verification. J Compo Mater. 2000;34(13):1081–116.